

## Ag/TiO<sub>2</sub>-SiO<sub>2</sub> Sol Gel Nanoparticles to use in Hospital-Acquired Infections (HAI)

López T<sup>1,2</sup>, Jardon G<sup>1</sup>, Gomez E<sup>2</sup>, Gracia A<sup>1</sup>, Hamdan A<sup>1</sup>, Luis Cuevas J<sup>1\*</sup>, Quintana P<sup>3</sup> and Novaro O<sup>2,4</sup>

<sup>1</sup>Universidad Autónoma Metropolitana-Xochimilco, Nanomedicine Laboratory, Calzada del Hueso No. 1100, Coyoacán, Villa Quietud, C.P. 04960 D.F., México

<sup>2</sup>Universidad Nacional Autónoma de México, Physics Institute, Theoretical Physics Department, Circuito de la Investigación Científica Ciudad Universitaria, 04510, México

<sup>3</sup>Centro de Investigación y de Estudios Avanzados del IPN, Mérida. Applied Physics Department. Antigua carretera a Progreso Km 6, Cordemex, 97310 Mérida, Yucatán, México

<sup>4</sup>El Colegio Nacional, Donceles 104, Centro Histórico, D.F., México

### Abstract

In this work utilizing sol-gel process we synthesized Ag/TiO<sub>2</sub>-SiO<sub>2</sub> nanomaterial containing 0.1, 1.0, 5.0, and 10% weight of silver. The samples were characterized with infrared (FTIR), Ultraviolet-visible (UV-VIS), Scanning Electron Microscopy (SEM), Z-Sizer and N<sub>2</sub> adsorption-desorption. The Nanoparticles (NPs) were tested in ten different types of strains by studying Kirby-Bauer susceptibility. The results show that the nanoparticles exhibit antimicrobial activity at all concentrations. We determinate de Minimum inhibitory concentration (MIC) which shown that *Candida albicans* ATCC 10231 and *Staphylococcus epidermidis* NRS 101 showed the highest sensitivity to silver NPs at concentrations of 10 and 1%.

**Keywords:** Nanomedicine; Ag-TiO<sub>2</sub>/SiO<sub>2</sub>; Sol-gel; Nosocomial infections; Antibacterial activity

### Introduction

A nosocomial infection, also called “Hospital-Acquired Infection (HAI)” can be defined as: an infection occurring in a patient in a hospital or other health care facility in whom the infection was not present or incubating at the time of admission [1]. Nosocomial infections occur worldwide and affect both developed and resource-poor countries. Infections acquired in health care settings are among the major causes of death and increased morbidity among hospitalized patients. They are a significant burden both for the patient and for public health [1]. Many patients receive antimicrobial drugs. Through selection and exchange of genetic resistance elements, antibiotics promote the emergence of multidrug resistant strains of bacteria; microorganisms in the normal human flora sensitive to the given drug are suppressed, while resistant strains persist and may become endemic in the hospital. The widespread use of antimicrobials for therapy or prophylaxis (including topical) is the major determinant of resistance. Antimicrobial agents are, in some cases, becoming less effective because of resistance. As an antimicrobial agent becomes widely used, bacteria resistant to this drug eventually emerge and may spread in the health care setting. Many strains of pneumococci, staphylococci, enterococci, and tuberculosis are currently resistant to most or all antimicrobials which were once effective [1].

Due to high resistance of the bacteria, new alternatives have been developed using Ag supported in TiO<sub>2</sub>-SiO<sub>2</sub> prepared by the sol-gel method as precursor. It has been proven that the new compounds are highly toxic to microorganisms in about 16 major bacterial species [2,3]. Especially SiO<sub>2</sub>-TiO<sub>2</sub> doped with silver forms nanoparticle (nanoAg-hospital) have recently received considerable attention, due to their antimicrobial capabilities [4-6]. These nanoAg-hospital reduce the growth of microorganisms (over 99%), has antifungal effects and good antibacterial activity against *Staphylococcus aureus* and *Escherichia coli* [7-9] and many others [10].

Many authors have used TiO [11-14], SiO<sub>2</sub> [15,16] or mixed oxides such as TiO<sub>2</sub>-SiO<sub>2</sub> [6,17] as support. In this paper, we synthesized Ag/TiO<sub>2</sub>-SiO<sub>2</sub> nanomaterials (nanoAg-Hospital) containing 0.1, 1.0, 5.0, and 10% weight of silver using sol-gel process [18,19]. Of key

importance is the interaction between the host matrix and Ag. These interactions occur primarily through the hydroxyl groups of host via hydrogen bridges, oxygen vacancies, free electrons and dipole attractions. These materials were studied by N<sub>2</sub> Adsorption-Desorption, Polydispersity index (PDI), Diffuse Reflectance (ERDT), FTIR, UV-vis spectroscopies, SEM, TGA and DRX.

### Materials and Methods

#### Chemical duty

- Deionized water
- Titanium tert-butoxide (Strem Chemical, 98% in butanol)
- Tetraethyl orthosilicate (Sigma Aldrich, 99.9%)
- Silver nitrate (Sigma Aldrich, 99.0%)
- Ammonium sulfate (Sigma Aldrich 99.0%)
- Absolute ethylic alcohol (J.T: Baker 99.9%)
- Gamma-Aminobutyric Acid (Sigma 99.0%)

Ag/TiO<sub>2</sub>-SiO<sub>2</sub> at 0.1, 0.5, 1.0, 5.0 and 10% in weight were prepared by the sol gel method (Figure 1). We used the required amounts of reagents to obtain 25 g of NPs. In a glass reflux system at room temperature, we added deionized water, silver nitrate, Gamma-aminobutyric acid and ammonium sulfate with constant stirring. Afterwards, titanium ter-butoxide mixed with an appropriate amount of ethanol and tetraethoxysilane (TEOS) were added drop by drop during four hours.

**\*Corresponding author:** Luis Cuevas J, Universidad Autónoma Metropolitana-Xochimilco, Nanomedicine Laboratory, Calzada del Hueso No. 1100, Coyoacán, Villa Quietud, C.P. 04960 D.F., México, Tel: 52 55 5483 7000; E-mail: [vjcuevasf@gmail.com](mailto:vjcuevasf@gmail.com)

**Received** August 21, 2015; **Accepted** September 03, 2015; **Published** September 13, 2015

**Citation:** López T, Jardon G, Gomez E, Gracia A, Hamdan A, et al. (2015) Ag/TiO<sub>2</sub>-SiO<sub>2</sub> Sol Gel Nanoparticles to use in Hospital-Acquired Infections (HAI). J Material Sci Eng 4: 196. doi:10.4172/2169-0022.1000196

**Copyright:** © 2015 López T, et al. This is an open-access article distributed under the terms of the Creative Commons Attribution License, which permits unrestricted use, distribution, and reproduction in any medium, provided the original author and source are credited.

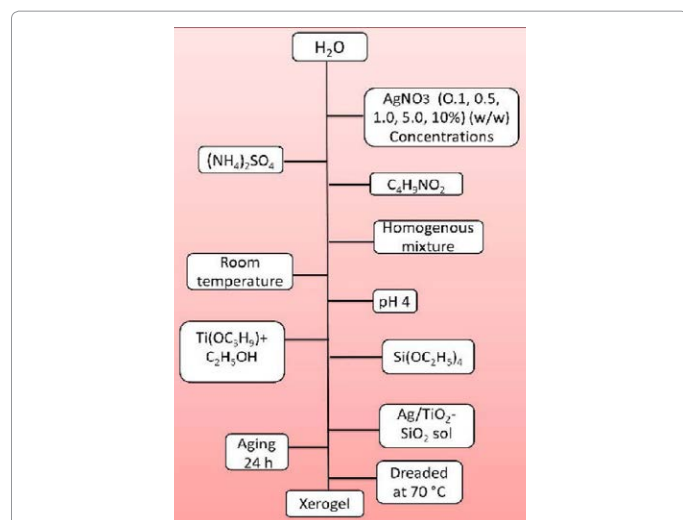


**Figure 1:** Diagram of preparation of Ag/TiO<sub>2</sub>-SiO<sub>2</sub> nanoparticles through sol-gel method.

After that, the constant stirring was maintained for 24 hours until gel formation. Finally, water and alcohol were removed at 70°C, to obtain completely dry nanostructured materials. The agglomerates NPs were weighted and were taken to a process of manual grinding in an agate mortar until a fine powder is obtained (Figure 1).

### Characterization

**N<sub>2</sub> adsorption-desorption:** the specific surface areas of all materials were calculated from N<sub>2</sub> isotherms, obtained with a BEL Japan Inc. apparatus. The samples were previously degassed under vacuum at 50°C for 2 h. The software BelprepII was used. The BET and BJH methods were used to calculate the specific area, the mean pore diameter and volume of pore.

**Polydispersity index (PDI):** PDI of the nanoAg-Hospital agglomerates was determined by techniques of dynamic light scattering (DLS) measurements performed at 25°C, using an equipment with dynamic laser light scattering (Z-sizer Nano-ZS, Malvern Instruments) equipped with a He-Ne laser (633 nm) and a digital correlator, model ZEN3600. All measurements were performed using water as a dispersing agent, who presented a polydispersity index of 1.33.

**FTIR spectra:** Spectra were recorded in the wavenumber region 400-4000 cm<sup>-1</sup>, on IR-affinity 1 (Shimadzu) Wafers were obtained by mixing 10% of each material with 90% of KBr.

**Diffuse Reflectance Spectroscopy (ERDT):** The absorbance of the materials in solid was determined using wavelengths from 200 to 800 nm. SCINCO® UV equipment, model S-3100, equipped with a diffuse reflector model SA-13.1 was used for this technique.

**Scanning Electronic Microscopy (SEM):** Was made in an equipment SEM-JEOL to 10 Kv. The sample was observed under high vacuum without pretreatment to a working distance of 10 mm.

**Evaluation of antimicrobial activity:** Susceptibility testing was performed by the following steps outlined in the Kirby-Bauer study, adopted by the National Committee for the Standardization of Laboratory, disk diffusion, then proceed as follows: 9 strains of bacteria and one strain were selected and one fungus, provided by the Laboratory of "Molecular Biology and Microbiology" at the Autonomous Metropolitan University. Later an inoculum reached 0.5 absorbance

O.D. in McFarland corresponds to 108 CFU / ml and seeded was prepared by method groove surfaces of Petri dishes containing Muller-Hinton agar. Sterile swabs were used for seeding Sensi-Discs 0.6 cm in diameter were placed, previously soaked in a suspension of each of the synthesized NPs and controls (7 Sensi-Discs per box). Suspensions together with soaked Sensi-Discs, left in constant stirring for 2 h before being placed in Petri dishes. Once placed, the plates were incubated at 37°C for 24 h. Finally the size of the halo of inhibition was determined using a ruler and account colonies to allow better visualization of the plates, the method was standardized to evaluate the antimicrobial activity at 150 ppm silver and a second experiment was conducted from the concentration minimum inhibitory obtained.

### Results and Discussion

Figure 2 shows that particles in sizes ranging from 0.2 μm to 1 μm in diameter, the smaller particles are observed in groups of high symmetry and agglomerates have a spherical appearance. Particles about 1 μm in diameter form aggregates as shown in Figure 2a, it is noteworthy that the image corresponding to this sample was treated with a gold coating, allowing better resolution when viewed under a microscope. Groups of agglomerates are constant in all synthesized nanoparticles, and its appearance is independent of the amount of silver contained. While there is not complete uniformity in all materials, particles smaller than 1 μm, are deposited on the periphery of the agglomerates (Figure 2b). Better visualization of this effect, shown in Figure 2c where ≈200 nm spherical particles are found on the edge of the agglomerate. In the micrograph corresponding to the matrix composed only by mixed oxide, TiO<sub>2</sub>-SiO<sub>2</sub>, no agglomerates (Figure 2d) are appreciated and have completely irregular shapes.

### Z sizer

Figure 3 shows that the average size of the particles obtained through technical dynamic light scattering of the three samples tested after a third analysis cycle, vary widely. Any polydispersity index (PDI) is close to 1, indicating that there is no uniformity in particle size. The Ag/TiO<sub>2</sub>-SiO<sub>2</sub> (5.0%) sample showed the highest variation after the third cycle, around 50%. With this technique it is only possible to determine the average size of a single type of particle in dispersion, that is, in all cases, these particles correspond to "microparticles" that are responsible for the formation of agglomerates and are comprised of hundreds of smaller structures. Table 1 shows the reading obtained after three cycles and the Ag concentration of each cycle.

### UV- vis

UV- vis absorption spectrum can be seen in Figure 4. In the spectrum of TiO<sub>2</sub>-SiO<sub>2</sub> one can see a peak around 334 nm due to electronic transitions in the titania from the 2p electrons in the atom of oxygen to the 3d electrons of titanium atom. When silver oxide is added in small amounts to the TiO<sub>2</sub>-SiO<sub>2</sub>, appear the prominent peak between 350-300 nm. The peaks of the high energy have bigger silver concentration. Nevertheless, when the quantity of silver is small the peaks are shifted to lower energy values. This phenomena can be explained, because the Ag<sub>2</sub>O is a tridimensional polymer with covalent bonds linking the metal with the oxygen and form easily hydrogen bridges with the hydroxyl groups of the network.

In Figure 5 is observed the presence of a TiO<sub>2</sub> bond at 800 cm<sup>-1</sup>, this range is characteristic of O-Ti-O vibrations [20]. This is a signal, characteristic of the stretching of the matrix also observed and consists of a mixed oxide: SiO<sub>2</sub>-TiO<sub>2</sub> (985 cm<sup>-1</sup>), this feature of materials derived from mixed oxides, has been reported by several authors, indicating

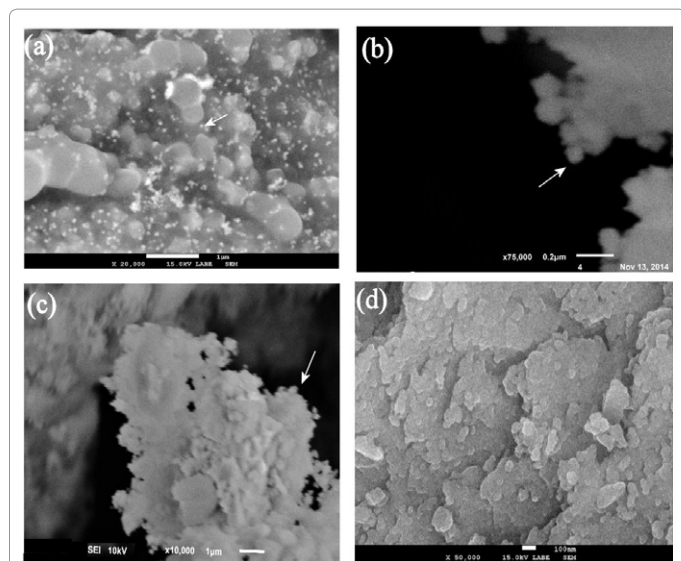


Figure 2: SEM images Ag/TiO<sub>2</sub>-SiO<sub>2</sub> of agglomerate of particles.

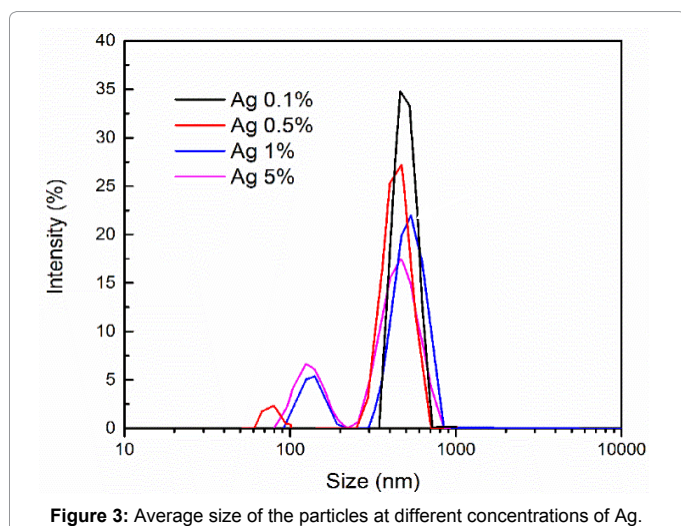


Figure 3: Average size of the particles at different concentrations of Ag.

that the titania form bonds with the silica matrix [21]. Furthermore, a higher band at 1100 cm<sup>-1</sup>, characteristic vibrating silica is observed. In this spectrum the presence of signals characteristic of OH bonds, adsorbed to the network of silica and titania, is observed. The formation of these bonds is attributed to the synthesis process, because the drying of the gel not involved calcining materials, but under mild conditions, whereby certain water molecules remain trapped within the network.

### N<sub>2</sub> adsorption-desorption isotherms

All the synthesis materials have IV isotherms. By UAPAC standards this type of isotherms are characteristics of mesoporous materials (with diameters 2 and 50 nm) in which, at low pressures a monolayer of adsorbate is formed in the pores surface. Thenceforth multiple layer follows. The increment of the pore volume up to P/Po≈0.45-0.65, can be ascribed to the filling up of N<sub>2</sub> in the mesoporous. On the other hand, the increase to P/Po beyond 0.9 is due to filling up of N<sub>2</sub> in the holes generated within the particle agglomerates.

This type of isotherms are quite important, they present hysteresis phenomenon. The sample Ag 5.0% has a H<sub>2</sub> type hysteresis characteristic

of nanomaterials with a well-defined pore size distribution This type of hysteresis is broader than the other cycles. The rest of the samples have a thin cycle or else hysteresis is difficult to observe.

Table 2 shows the results of the BET analysis, which shows that Ag 5% sample, has the highest surface area (390 m<sup>2</sup>/g) and average pore diameter (5.4848 nm). This result indicates that the increase in silver provokes that the area and pore size increase. On the other hand for Ag 10%, the specific surface area and the average pore collapses (Figure 6).

### Analysis of the pore size distribution

To calculate the diameter of the pores and its size distribution, the traditionally used BJH method is applied to the adsorption phase. There is ample evidence that the latter underestimates the pore size due to the Kelvin equation in which the model is based and does not consider the adsorbent-adsorbate interactions. This research was limited to the application of the traditional methodology, by the BJH method, which despite giving sizes rather lower than the actual ones, provides a rough idea of the size distribution. The above graphs show that the synthesized nano-materials have heterogeneous distribution diameters. This can be attributed to the network's disorder due to the presence of anatase of both tetraedical and octahedral silica. Furthermore, there are punctual defects: oxygen vacancies, hydroxyl groups on the external and internal surface; as well as hydrogen bridges between the silver compound and the network. For materials with different concentrations of Ag pore sizes of less than 2 nm occur, which indicates the presence of a few micropores (Figure 7 and Table 3).

| Cycle                          | 1             | 2             | 3             | % Ag |
|--------------------------------|---------------|---------------|---------------|------|
| Size of the nanoparticles (nm) | 1366 ± 13.6   | 1015 ± 10.15  | 975.3 ± 9.7   | 0.1  |
|                                | 1452 ± 14.5   | 1133 ± 11.33  | 734 ± 7.37    | 0.5  |
|                                | 1232 ± 12.3   | 1203 ± 12.03  | 771 ± 7.7     | 1    |
|                                | 1231 ± 12.3   | 774.4 ± 7.7   | 503.3 ± 5     | 5    |
| Polydispersity index (Pdl)     | 0.902 ± 0.009 | 0.720 ± 0.007 | 0.662 ± 0.006 | 0.1  |
|                                | 0.822 ± 0.008 | 0.728 ± 0.007 | 0.636 ± 0.006 | 0.5  |
|                                | 0.801 ± 0.008 | 0.791 ± 0.007 | 0.602 ± 0.006 | 1    |
|                                | 0.868 ± 0.008 | 0.773 ± 0.007 | 0.512 ± 0.005 | 5    |

Table 1: Size of the particles and polydispersity index at different concentration of Ag.

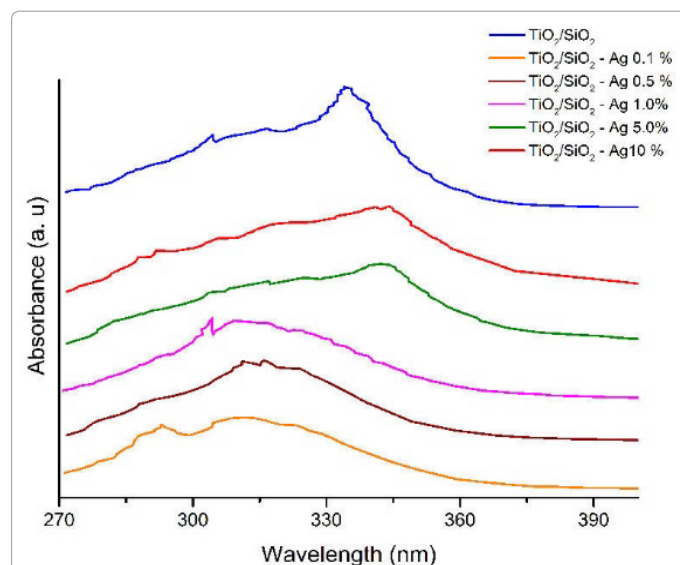


Figure 4: UV-Vis spectra and characteristic signals of TiO<sub>2</sub>-SiO<sub>2</sub> with different concentrations of Ag.

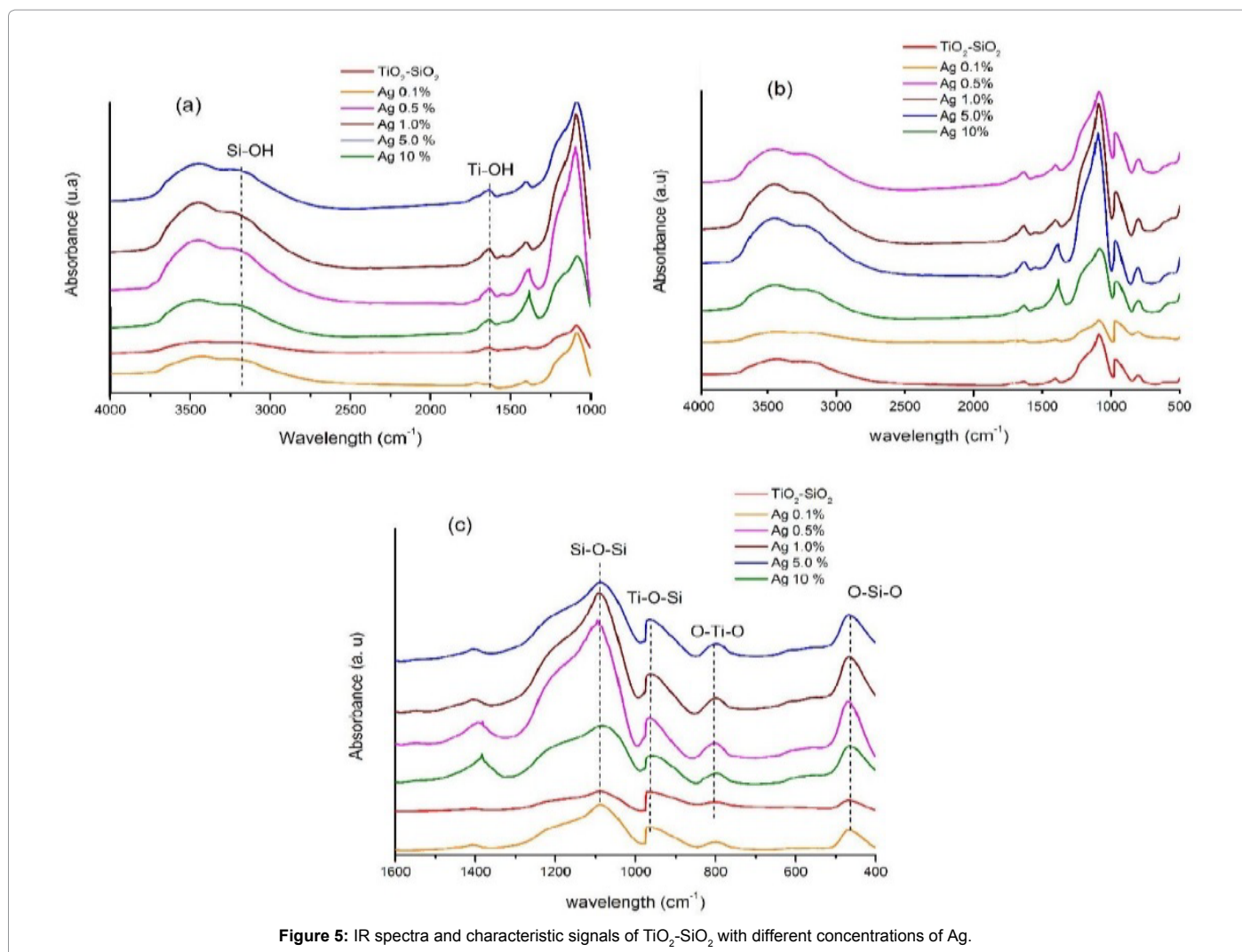


Figure 5: IR spectra and characteristic signals of TiO<sub>2</sub>-SiO<sub>2</sub> with different concentrations of Ag.

| Sample                                       | surface area (m <sup>2</sup> /g) | Average Pore Diameter (nm) |
|--|----------------------------------|----------------------------|
| Ag/TiO <sub>2</sub> -SiO <sub>2</sub> (0.1%) | 162 ± 24.3                       | 3.2 ± 0.4                  |
| Ag/TiO <sub>2</sub> -SiO <sub>2</sub> (0.5%) | 281 ± 42.1                       | 2.9 ± 0.4                  |
| Ag/TiO <sub>2</sub> -SiO <sub>2</sub> (1.0%) | 348 ± 52.2                       | 3.7 ± 0.5                  |
| Ag/TiO <sub>2</sub> -SiO <sub>2</sub> (5.0%) | 390 ± 58.5                       | 5.4 ± 0.8                  |
| Ag/TiO <sub>2</sub> -SiO <sub>2</sub> (10 %) | 245 ± 36.7                       | 3.2 ± 0.4                  |

Table 2: BET and BJH average pore diameter of the nanoparticles synthesized.

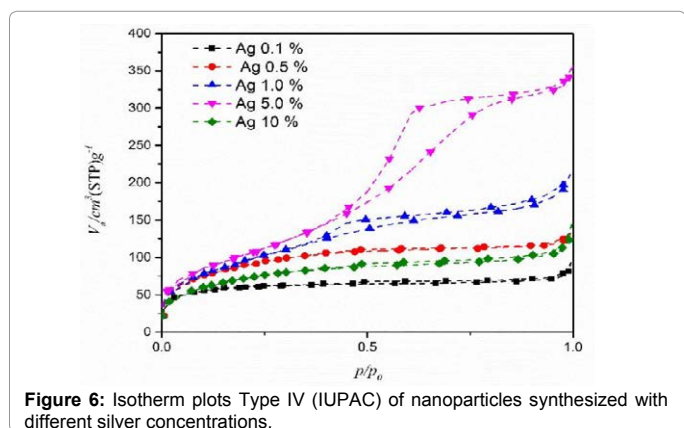


Figure 6: Isotherm plots Type IV (IUPAC) of nanoparticles synthesized with different silver concentrations.

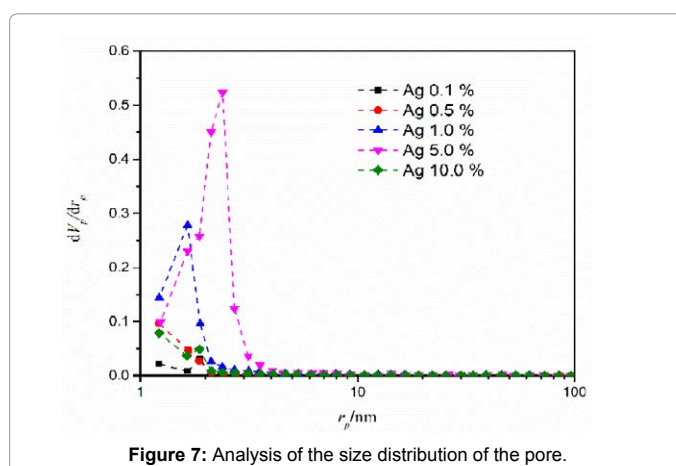


Figure 7: Analysis of the size distribution of the pore.

### Antimicrobial activity

Table 4 shows the inhibition halos generated by nanoparticles synthesized with different percentages of silver used in suspension at a concentration of 150 ppm of silver occurs. All different concentrations of Ag nanoparticles showed antimicrobial activity against both Gram

| Simple                                       | Pore volume (V <sub>p</sub> ) (cm <sup>3</sup> /g) | Pore mean diameter (D <sub>p</sub> ) (nm) | Specific surface Area (m <sup>2</sup> /g) |
|--|--|---|---|
| Ag/TiO <sub>2</sub> -SiO <sub>2</sub> (0.1%) | 0.0591 ± 0.005                                     | 3.4 ± 0.34                                | 38 ± 3.8                                  |
| Ag/TiO <sub>2</sub> -SiO <sub>2</sub> (0.5%) | 0.1165 ± 0.011                                     | 1.4 ± 0.14                                | 130 ± 13                                  |
| Ag/TiO <sub>2</sub> -SiO <sub>2</sub> (1.0%) | 0.2827 ± 0.028                                     | 2.6 ± 0.26                                | 280 ± 28                                  |
| Ag/TiO <sub>2</sub> -SiO <sub>2</sub> (5.0%) | 0.5804 ± 0.058                                     | 5.6 ± 0.56                                | 528 ± 52.8                                |
| Ag/TiO <sub>2</sub> -SiO <sub>2</sub> (10%)  | 0.1485 ± 0.014                                     | 1.4 ± 0.14                                | 120 ± 12                                  |

Table 3: Data of the size distribution by BJH method.

| Strains/ Concentration                  | 0.10%    | 0.50%    | 1.00%    | 5.00%    | 10.00%   | Reference SiO <sub>2</sub> -TiO <sub>2</sub> |
|---|----------|----------|----------|----------|----------|--|
| <i>E. coli</i> ATCC 10586               | 12 ± 1.2 | 13 ± 1.3 | 12 ± 1.2 | 12 ± 1.2 | 16 ± 1.3 | 0  |
| <i>Klebsiella pneumoniae</i> ATCC 10031 | 11 ± 1.1 | 13 ± 1.3 | 12 ± 1.2 | 15 ± 1.5 | 14 ± 1.3 | 0  |
| <i>P. mirabilis</i>                     | 9 ± 0.9  | 9 ± 0.9  | 9 ± 0.9  | 11 ± 1.5 | 13 ± 1.3 | 0  |
| <i>P. vulgaris</i>                      | 10 ± 1   | 13 ± 1.3 | 11 ± 1.1 | 12 ± 1.2 | 13 ± 1.3 | 0  |
| <i>Salmonella enterica</i> ATCC 14028   | 12 ± 1.2 | 13 ± 1.3 | 12 ± 1.2 | 12 ± 1.2 | 15 ± 1.5 | 0  |
| <i>P. aeruginosa</i>                    | 13 ± 1.3 | 14 ± 1.4 | 14 ± 1.4 | 14 ± 1.4 | 17 ± 1.7 | 0  |
| <i>S. aureus</i> ATCC 43300             | 10 ± 1   | 10 ± 1   | 12 ± 1.2 | 12 ± 1.2 | 11 ± 1.1 | 0  |
| <i>S. epidermidis</i> NRS 101           | 13 ± 1.3 | 13 ± 1.3 | 14 ± 1.4 | 14 ± 1.4 | 15 ± 1.5 | 0  |
| <i>E. faecalis</i> ATCC 29212           | 9 ± 0.9  | 14 ± 1   | 10 ± 1   | 10 ± 1   | 12 ± 1.2 | 0  |
| <i>C. albicans</i> ATCC 10231           | 13 ± 1.3 | 19 ± 1.9 | 19 ± 1.9 | 19 ± 1.9 | 19 ± 1.9 | 0  |

Table 4: Inhibition halos (mm) produced by suspensions of nanoparticles 150 ppm of at different silver concentrations.

| Strains/ Concentration                | 0.10%    | 0.50%    | 1.00%    | 5.00%    | 10.00%   | Reference SiO <sub>2</sub> -TiO <sub>2</sub> |
|---------------------------------------|----------|----------|----------|----------|----------|--|
| <i>E. coli</i> ATCC 10586             | 13 ± 1.3 | 12 ± 1.2 | 12 ± 1.2 | 12 ± 1.2 | 14 ± 1.4 | 0  |
| <i>K. pneumoniae</i> ATCC 10031       | 12 ± 1.2 | 12 ± 1.2 | 13 ± 1.2 | 12 ± 1.2 | 13 ± 1.2 | 0  |
| <i>P. mirabilis</i>                   | 13 ± 1.3 | 13 ± 1.3 | 14 ± 1.4 | 13 ± 1.3 | 13 ± 1.3 | 0  |
| <i>Salmonella enterica</i> ATCC 14028 | 12 ± 1.2 | 14 ± 1.4 | 15 ± 1.5 | 14 ± 1.4 | 14 ± 1.4 | 0  |
| <i>S. epidermidis</i> NRS 101         | 17 ± 1.7 | 17 ± 1.7 | 20 ± 2   | 19 ± 1.9 | 19 ± 1.9 | 0  |
| <i>P. aeruginosa</i> ATCC 2619        | 11 ± 1.1 | 12 ± 1.2 | 12 ± 1.2 | 12 ± 1.2 | 12 ± 1.2 | 0  |
| <i>Salmonella enterica</i> ATCC 14028 | 12 ± 1.2 | 14 ± 1.4 | 15 ± 1.5 | 14 ± 1.4 | 14 ± 1.4 | 0  |
| <i>S. aureus</i> ATCC 43300           | 11 ± 1.1 | 11 ± 1.1 | 12 ± 1.2 | 14 ± 1.4 | 14 ± 1.4 | 0  |
| <i>E. faecalis</i>                    | 10 ± 1   | 12 ± 1.2 | 12 ± 1.2 | 13 ± 1.3 | 13 ± 1.3 | 0  |
| <i>C. albicans</i> ATCC 10031         | 20 ± 2   | 21 ± 2.1 | 22 ± 2.2 | 24 ± 2.4 | 25 ± 2.5 | 0  |

Table 5: Inhibition halos (mm) produced by suspensions of nanoparticles 0.12077 g/mL of at different silver concentrations.

positive and negative bacteria, as well as the yeast *Candida albicans*. The larger halo inhibition observed was *Candida albicans* culture ATCC 10231, and remains for inhibition percentages of 0.5 to 10% Ag/TiO<sub>2</sub>-SiO<sub>2</sub> for the group of bacteria here studied. *Staphylococcus aureus* ATCC 43300 showed indeed of lower halos than the other bacteria. This microorganism is a major nosocomial infectious agent. In *Enterococcus faecalis*, nanoparticles with 0.5% silver produced the greatest inhibition halo. In *Pseudomonas aeruginosa* and *Staphylococcus epidermidis* 0.1% nanoparticles show the best silver halos of inhibition, this is important because it can be used silver nanoparticles at low concentrations in materials or medical devices.

In Table 5 we observe the inhibition halos for a higher concentration of AgNO<sub>3</sub>/TiO<sub>2</sub>-SiO<sub>2</sub>. Minor inhibition halos correspond to *Proteus vulgaris*, as well as *Pseudomonas aeruginosa* ATCC 2619. *Staphylococcus epidermidis* NRS 101 ATCC 14028 and *Salmonella enterica* require high concentration of Silver (1%). On the other hand *E. coli* ATCC 10586 can be attack with concentrations as low as 0.1%

## Conclusions

Due to the increase of bacterial resistance to antimicrobial agents, it is necessary develop new materials which will be biocompatible and nontoxic. Ag nanoparticles supported in TiO<sub>2</sub>-SiO<sub>2</sub> provide an effective treatment for Hospital-acquired infections. The results of this study

demonstrate that nanostructured sol-gel Ag/TiO<sub>2</sub>-SiO<sub>2</sub> has a bactericidal effect including highly pathogenic bacteria such as *Salmonella enterica* and *E. coli* ATCC 10586 which require around 1% and 0.1% of silver concentration. This fact impact directly in the production cost due to the smaller quantities of silver which is necessary for obtaining similar results using higher concentrations thereof.

## References

- Ducel G, Fabry J, Nicolle L (2002) Prevention of hospital-acquired infections a practical guide.
- Prabhu S, Poulouse EK (2012) Silver nanoparticles: mechanism of antimicrobial action, synthesis, medical applications, and toxicity effects. International Nano Letters 2:32.
- Berger TJ, Spadaro JA, Chapin SE, Becker RO (1976) Electrically Generated Silver Ions Quantitative Effects on Bacterial and Mammalian Cells. Antimicrobial Agents and Chemotherapy 9: 357-358.
- Dhanalekshmi KI, Meena KS (2014) Comparison of antibacterial activities of Ag@TiO<sub>2</sub> and Ag@SiO<sub>2</sub> core-shell nanoparticles. Spectrochim Acta A Mol Biomol Spectrosc 128: 887-90.
- Zhang Q, Ye J, Tian P, Lu X, Lin Y, et al. (2013) Ag/TiO<sub>2</sub> and Ag/SiO<sub>2</sub> composite spheres: synthesis, characterization and antibacterial properties. RSC Advances 3: 9739.
- Sun B, Sun S, Li T, Zhang W (2007) Preparation and antibacterial activities of Ag-doped SiO<sub>2</sub>-TiO<sub>2</sub> composite films by liquid phase deposition (LPD) method. Journal of Materials Science 42: 10085-10089.

7. Ahmadi F, Abolghasemi S, Parhizgari N, Moradpour F (2013) Effect of Silver Nanoparticles on Common bacteria in Hospital Surfaces. *Jundishapur Journal of Microbiology* 6: 209.
8. Kim SH, Lee HS, Ry DS, Cho SJ, Lee DS (2011) Antibacterial Activity of Silver-nanoparticles Against *Staphylococcus aureus*. *Korean Journal of Microbiology and Biotechnology* 39: 77-85.
9. Kim KJ, Sung WS, Suh BK, Moon SK, Choi JS, et al. (2009) Antifungal activity and mode of action of silver nano-particles on *Candida albicans*. *Biometals* 22: 235-242.
10. Buzea C, Pacheco II, Robbie K (2007) Nanomaterials and nanoparticles: Sources and toxicity. *Biointerphases* 2: MR17-MR172.
11. Zhang H, Chen G (2009) Potent Antibacterial Activities of Ag/TiO<sub>2</sub> Nanocomposite Powders Synthesized by a One-Pot Sol-Gel Method. *Environmental Science and Technology* 43: 2905-2910.
12. Lopez Goerne TM, Alvarez Lemus MA, Morales VA, Gómez López E, Castillo Ocampo P (2012) Study of Bacterial Sensitivity to Ag-TiO<sub>2</sub> Nanoparticles. *Journal of Nanomedicine & Nanotechnology* s5(01).
13. Badawy MI, Souaya EMR, Gad-Allah TA, Abdel-Wahed MS, Ulbricht M (2014) Fabrication of Ag/TiO<sub>2</sub> photocatalyst for the treatment of simulated hospital wastewater under sunlight. *Environmental Progress & Sustainable Energy* 33: 886-894.
14. Zhou W, Li T, Wang J, Qu Y, Pan K, et al. (2014) Composites of small Ag clusters confined in the channels of well-ordered mesoporous anatase TiO<sub>2</sub> and their excellent solar-light-driven photocatalytic performance. *Nano Research* 7: 731-742.
15. Kim YH, Lee DK, Gil Cha H, Woo Kim C, Kang YS (2007) Synthesis and Characterization of Antibacterial Ag-SiO<sub>2</sub> Nanocomposite. *Journal of Physical Chemistry C* 111: 3629-3635.
16. Wang HS, Wang C, He YK, Xiao FN, Bao WJ, et al. (2014) Core-shell Ag@SiO<sub>2</sub> nanoparticles concentrated on a micro/nanofluidic device for surface plasmon resonance-enhanced fluorescent detection of highly reactive oxygen species. *Anal Chem* 86: 3013-3019.
17. Chiu PK, Lee CT, Chiang D, Cho WH, Hsiao CN, et al. (2014) Conductive and transparent multilayer films for low-temperature TiO<sub>2</sub>/Ag/SiO<sub>2</sub> electrodes by E-beam evaporation with IAD. *Nanoscale Research Letter* 9: 35.
18. Asomoza M, Lopez T, Zamalloa A, Gomez R, Figueroa G (1992) Catalytic Activity and characterization of Pt/SiO<sub>2</sub> catalyst prepared by the sol-gel method. *New Journal of Chemistry* 16: 959-963.
19. Lopez T, Bosch P, Moran M, Gomez R (1993) Pt-SiO<sub>2</sub> Sol-Gel Catalysts Effects of pH and Platinum Precursor. *Journal of physical Chemistry* 97: 1671-1677.
20. López T, Ortiz E, Mezad D, Basaldellae E, Bokhimif X, et al. (2011) Controlled release of phenytoin for epilepsy treatment from titania and silica based materials. *Materials Chemistry and Physics* 126: 922-929.
21. Hui Pan, Wang XD, Xiao SS, Yu LG, Zhang ZJ (2013) Preparation and characterization of TiO<sub>2</sub> nanoparticles surface-modified by octadecyltrimethoxysilane. *Indian Journal of Engineering and Material Sciences* 20: 561-567.